Non-stoichiometric methanation as strategy to overcome the limitations of green hydrogen injection into the natural gas grid

Applied Energy 309 (2022) 118462

Contents lists available at ScienceDirect

Applied Energy

journal homepage: www.elsevier.com/locate/apenergy

Non-stoichiometric methanation as strategy to overcome the limitations of green hydrogen injection into the natural gas grid

Luis M. Romeo [a,*], Marco Cavana [b], Manuel Bailera [a], Pierluigi Leone [b], Begoña Peña [a], Pilar Lisbona [a]

[a] Escuela de Ingeniería y Arquitectura, Departamento de Ingeniería Mecánica, Universidad de Zaragoza, Zaragoza, Spain
[b] Politecnico di Torino, Dipartimento Energia "Galileo Ferraris", Torino, Italy

HIGHLIGHTS

- 300 kW electrolyser H_2 injection into the gas grid is non-compliant with quality requirements.
- If H_2 is converted in a non-stoichiometric methanation, SNG can be fully accepted.
- It leads to 3.3% natural gas savings without saturating network H_2 acceptability.
- Non-stoichiometric methanation H_2/CO_2 ratio is 5.6 for complete carbon conversion.
- This concept increases H_2 injection in gas networks and facilitates sector coupling.

ARTICLE INFO

Keywords:
Hydrogen
Gas grid
Natural gas
Power-to-gas
Partial methanation

ABSTRACT

The utilization of power to gas technologies to store renewable electricity surpluses in the form of hydrogen enables the integration of the gas and electricity sectors allowing the decarbonization of the natural gas network through green hydrogen injection. Nevertheless, the injection of significant amounts of hydrogen may lead to high local concentrations that may degrade materials (e.g. hydrogen embrittlement of pipelines) and in general be not acceptable for the correct and safe operation of appliances. Most countries have specific regulations to limit hydrogen concentration in the gas network. The methanation of hydrogen represents a potential option to facilitate its injection into the grid. However, stoichiometric methanation will lead to a significant presence of carbon dioxide, limited in gas networks, and requires an accurate design of several reactors in series to achieve relevant concentrations of methane. These requirements are smoothed when the methanation is undertaken under non-stoichiometric conditions (high H/C ratio). This study aims to assess to influence of non-stoichiometric methanation under different H/C ratios on the limitations presented by the pure hydrogen injection. The impact of this injection on the operation of the gas network at local level has been investigated and the fluid-dynamics and the quality of gas blends have been evaluated. Results show that non-stoichiometric methanation could be an alternative to increase the hydrogen injection in the gas network and facilitates the gas and electricity sector coupling.

1. Introduction

The foreseen massive deployment of renewable energy sources will be followed by important challenges related to the management of the grid and the electric sector such as the development of highly efficient energy storage systems or the proper integration of renewable technologies in the generation mix, safeguarding security and economic balance [1,2].

In this future scenario, a promising option to overcome the intermittency of energy production and production-consumption mismatching is the implementation of Power to Fuel technologies [3]. These technologies store energy surpluses to be used in the future by means of producing a synthetic fuel. Hydrogen is the most common one given the lower energy penalty of its production process but there exist also other low net carbon emissions gas energy fuels, the so-called renewable gases [4]. Biogas, biomethane, syngas, hydrogen and synthetic natural gas

* Corresponding author.
E-mail address: luismi@unizar.es (L.M. Romeo).

https://doi.org/10.1016/j.apenergy.2021.118462
Received 22 July 2021; Received in revised form 13 November 2021; Accepted 25 December 2021
Available online 10 January 2022

(SNG) belong to this category. The main barriers to make this process feasible are the high investment, the change in infrastructures and the relatively low round-trip efficiency [5]. This alternative overcomes one of the main disadvantages of present energy storage technologies, their low capacity. Gas network infrastructure has been considered in the latest years as a possible storage reservoir of renewable energy with a remarkable potential and a distributed feature [6]. The hydrogen production through Power to Fuel and subsequent blending within the already existent gas infrastructure is an example of electricity and gas sectors coupling [7] and it is considered an innovative and effective decarbonisation option.

The European Commission published the hydrogen strategy for a climate-neutral Europe [8] to define a precise roadmap towards 2030 and 2050 for a creation of a complete hydrogen ecosystem. Along with these policy statements, a report released by several European natural gas TSOs proposes a roadmap for a fully developed hydrogen infrastructure on continental level [9]. While the goal is to build up a 100% hydrogen infrastructure by late 2040s – 2050, the hydrogen blending is considered an earlier option (already for the 2020s) to deploy hydrogen in the pipeline.

However, a number of technical aspects are still to be addressed given the large differences of hydrogen physical and chemical properties with respect to natural gas. An extensive review of the opportunities and criticalities of hydrogen admixture within the current gas infrastructure is given in [10]. Hydrogen has completely different properties than natural gas and its presence has an impact on all the levels of the involved infrastructure. The main concerns related to direct injection of hydrogen into the natural gas network are the following:

1. Detrimental effects on the infrastructure materials such as embrittlement [11]. It is related in iron and steel pipes and cause the propagation of cracks in the pipework [12]. However, the presence of hydrogen affects only slightly the mechanical properties [13]. This is true for most of the materials employed in pipes, included copper pipes at indoor piping systems [14].
2. Gas leakages. Hydrogen has a propensity to leak from connections between fittings and from sealants [15]. Although the leakage rates would not be high enough to be a major concern [10], it represents an energy loss and may requires revisions on the usual detection protocols and risk management assessments.
3. Safety. Hydrogen has a wider flammability range due to the much higher flammability limit than natural gas (75% versus 14%). However, the impact on flammability ranges of hydrogen-natural gas blends is minor as long as hydrogen shares little: at 30% hydrogen the upper flammability limit of the blend is 20%. As for the lower flammability limit, it is unvaried as both for hydrogen and natural gas it is about 4%. This reduces the impacts on odorization requirements. What is more, it has been proved that hydrogen does not interact with THT [16] and TBM [17], the most common odorants in the infrastructure. In the end, given the larger flammability range and lower ignition energy required to hydrogen, some studies recommended threshold concentrations up to 15–20% hydrogen blend by volume (vol%) [18].
4. Quality management of the gas flows. Adding hydrogen to natural gas pipelines reduces the energy delivery of the grid (on volumetric basis). The effects are nonlinear and depend primarily on the flow properties of the hydrogen [19]. As hydrogen is also less compressible than natural gas, the effect becomes more pronounced at higher pressures.
5. Final users' appliances. Hydrogen presence impacts on the final users' appliances, with different degrees of severity according to the type of appliances themselves. Maximum values of admissible hydrogen concentrations are given for a number of different natural gas systems [20].
6. Gas meters and pressure regulators may also be impacted by hydrogen presence. However, according to [21] gas meters do not experience significant metrological differences for concentration up to 20%. In [22] a slight undercounting is registered but it is still within the range of the specification of EN 1359. This phenomenon is more evident in diaphragms meters, maybe related to the impact of hydrogen on elastomeric materials.
7. Underground gas storage. Hydrogen presence within the natural gas may have potentially detrimental effects such as leakages, biochemical reactions and interferences with minerals in the geological formations [23].

All these aspects have not been solved and they are the reasons behind the lack of consensus or indication on the allowable limit of hydrogen presence within the current infrastructure within the current technical norms and standards. The norm EN 16726:2019 [24] on standardisation of gas quality (group H) mentions the possibility of hydrogen injection but recommends a case by case analysis to establish its acceptability. Thus, there are no unified international or European regulations to define the admissible concentrations in the natural gas grid: European regulators usually does not define thresholds on single natural gas component (e.g. hydrogen) but rather on relevant gas quality parameters such as the higher heating value, the relative density and the Wobbe Index. This is the case of the Italian gas network [25]. Other regulators limit the amount of hydrogen in the grid between 0.1 and 10% in volume depending on the country [26]: the most advanced technical regulation considers the injection up to 10% of hydrogen blended with natural gas in Germany in the case there are no compressed natural gas (CNG) stations in the network. The limit in France is 6%, Austria 4% and Switzerland has a limit set at 2%. All these limits are expressed in terms of volume concentrations. Spain, similarly to Italy, does not set any limit to the hydrogen concentration within natural gas but it limits the hydrogen presence to a 5 $\%_{vol}$ in the case of unconventional gases injection [27]. In Italy, the acceptable hydrogen content within biomethane is limited to 1% $_{vol}$ [28]. In general, the massive blending of pure hydrogen is not possible yet: very few countries allows the direct injection of pure hydrogen within the infrastructure [29].

Gas quality variations within the gas networks have been recently studied because of the growth of wider international interconnections brought by LNG and renewable gas uptake. The effect of hydrogen injection into the natural gas system will have a strong influence in the variation of gas quality along the network. Generally, these studies consider a variable gas quality and make use of steady state equations for fluid-dynamic simulations of networks topology. The simulations of distributed injection of renewable gas on a urban level distribution system (low pressure) [30] and on a regional transmission network (high pressure) [31] highlight the impacts of hydrogen on the gas quality and determine the maximum amount of renewable energy which is storable within the network in the form of hydrogen [31]. However, time-dependent simulations are needed in order to grasp the complexity of intersectoral transfer of renewable energy through power-to-hydrogen and hydrogen blending.

The use of dynamic gas network models which implements also quality tacking features as the one presented in [32,33] are important to quantify the time evolution of hydrogen concentration at any node of the grid, for different injection flowrates and consumption scenarios. They allow the detection of peak concentrations in specific areas of the grid and also enable to determine the acceptable injection rate of hydrogen in order to comply with gas quality requirements [34]. This approach highlights the limitations to the integration between power and gas sector imposed by the gas system, which, at least for now, lays boundaries to the hydrogen presence and hydrogen variability.

As an alternative to direct injection of pure hydrogen and to extend the application of hydrogen as energy vector, its combination with CO_2 to produce other renewable gases has been proposed. A particular solution could be its methanation through Sabatier's reaction [3]. This concept uses the stored hydrogen to produce methane via the methanation of CO_2 ($CO_2 + 4H_2 \leftrightarrow CH_4 + 2H_2O$). The methanation is an

exothermic reaction (1.8 kWh/Nm^3CH_4). Differently from hydrogen, methane does not present any major problem to be injected into the natural gas grid. The only disadvantages come from its limited potential for significantly reducing CO_2 emissions in the long term [11] as CO_2 will be released again in its usage stage [35] unless it will be used cyclically [36,37].

Several works analysed the Power to Gas for injection into the gas grid. Some reviews of projects, technological and economical review and lesson learned are found in literature [3,5]. By integrating power-to-gas with the natural gas grid, it is possible to exploit the inherent flexibility of the grid, and shift some electricity variability onto the gas grid. Some works have reviewed power-to-gas for injection into the gas grid, as this application has specific economic, technical and modelling opportunities and challenges and they have identified both, interests and challenges to overcome and find profitable business cases [11]. The potential of Power to Gas has been modelled when combined with gas seasonal storage operation accounting for the two networks' characteristics and constraints [38]. Blending of produced hydrogen from renewable energy resources into the gas grid has been promoted as a viable means of energy transportation and long-time storage in large-scales [39]. The Power to Methane process requires a CO_2 source which should be taken into account in the technical and economic assessment [40]. Together with the dynamic behaviour of the individual process steps, the economics and the system efficiency, the availability of CO_2 sources and final gas quality are some of the critical aspects for Power to Gas processes [5]. Regarding gas quality, the methanation reaction usually is not complete [5,41]. Increasing system pressure positively influences the reaction, because it shifts the equilibrium CO2 conversion [42,43]. Pressures of 10 bars have been considered in theoretical calculations [42] of fixed beds and electrolysed could produce hydrogen also at higher pressures. It increases the process complexity and equipment cost and for this reason an atmospheric methanation has been considered. A complete analysis for specific applications that include H_2 production, CO_2 source and CH_4 utilization is needed to determine the optimum operational pressure of the methanation stage.

Typical composition of the synthetic gas produced through methanation under stoichiometric H/C conditions, with 0.7 recycle ratio to methanation reactor and high pressure (20 bar) and temperatures (260–550 °C) may reach 95.9% of CH_4, 3.3% H_2 and 0.8% CO_2 [44]. When the methanation reactor operates at atmospheric pressures, the typical equilibrium composition of syngas from the process in this range of temperatures is modified with a rapid decay of methane content between near 96% of CH_4 for 260 °C and 68% for 550 °C and significant presence of carbon dioxide [45].

The novelty of this study is the application of non-stoichiometric methanation at atmospheric pressure, with ratio H/C higher than 4.0, to avoid the injection of pure hydrogen into the natural gas grid converting the renewable gas into a variable mixture of hydrogen and methane. This partial transformation of hydrogen into methane allows for the reduction of hydrogen concentration in the grid (that are evaluated in this study), and the consequent removal of the issues affecting the gas system listed above, while storing in the gas network nearly the same amount of renewable energy coming from the power to hydrogen pathway. With respect to previous works on the modelling of injection of hydrogen (such as [33]), in this paper the concept has been extended to SNG. The efficiency losses in the transformation from hydrogen to synthetic methane are prevented by the novel proposed operations of the methanation unit. Since the complete conversion of hydrogen into methane is not required, the complexity of methanation reactors is reduced and the presence of CO_2 in the produced syngas is avoided. The use of large H/C ratios facilitates the complete conversion of carbon in a single-step methanation fixed-bed reactor making easier the design, control and operation of the process as well as its economic feasibility.

The present work has two main objectives. Firstly, to experimentally demonstrate the feasibility of the concept and to quantify the optimum ratio of H/C to achieve complete carbon conversion and suitable hydrogen concentrations. Secondly, it seeks the assessment, through simulation of the natural gas grid, of the mass flow rate limitations when pure H_2 is injected into the grid compared to the injection of a mixture of H_2/CH_4 coming from the non-stoichiometric methanation of the same amount of hydrogen. The obtained results prove the benefits of the proposed concept for introducing renewable energy into the gas grid without restrictions provided that gas quality constraints are globally set at the network level and not at injection point.

2. Methanation test facility and experimental tests

2.1. Experimental facility

The lab-scale methanation facility is shown in Fig. 1. The main equipment is the fixed bed, plug flow reactor, analogous to those tested in the literature [46,47] or proposed in simulations for small scale applications [42]. In addition, the facility includes a ceramic heater to preheat the mixture of reactants up to 250–350 °C with a pressure of 3 bar just before the CO2 and H2 mass controllers, a condenser coil to remove the produced water and a burner to oxidize the resultant fuel mixture (H_2 and CH_4) together with bottled butane [41,48]. Additionally, there is a N_2 input before the ceramic heater for cleaning and heating purposes.

The reactor has electrical heating and air cooling to control the reaction temperature. It consists of a concentric pipe with parallel flows, being 100 mm the outer diameter of the shell. The reaction takes place in the inner duct where the catalyst is located, while the cooling air flows through the outer annular space. A commercial Ru-based catalyst (Sigma-Aldrich 206199) has been used in the form of pellets of alumina impregnated with Ruthenium (0.5 wt% Ru/Al_2O_3), supported by quartz wool. The fixed bed is located inside the tube of 590 mm height, 33.4 mm inner diameter and 4.45 mm thickness. The reactants (H_2 and CO_2) are supplied from bottles to avoid undesired impurities inside the reactor.

Standard instrumentation of pressure, temperature and mass flow is installed at strategic points of the facility. Specifically, the reactor inlet and outlet pressures and temperatures are measured for the reactants and the cooling air, while nine thermocouples evenly distributed (5 cm of separation) register the temperature of the reactor wall (the inner pipe). Two mass flow controllers for H_2 and CO_2 allows adjusting the mass fractions to the desired H/C ratio before the gas preheating. Then, the composition of the reactive mixture is measured through a gas analyzer before the methanation reactor. The gas analyzer comprises two units of Siemens: "CALOMAT 6" for the H_2 content (measured by thermal conductivity), and "ULTRAMAT 23" for CO, CO_2 and CH_4 (infrared detector). After methanation stage, the resultant flow is driven to a condenser to reduce the water content and the outlet gas composition is also measured. Finally, the produced fuel is burnt in a butane pilot flame.

An advanced Labview system allows for the supervision of the process, the control of the reactants mass flows and the recording of all the measurements for further analysis.

2.2. Tests description

The lab-scale experimental plant was run to find stationary operation points which lead to steady carbon conversions in the reactor and approximately constant temperatures at the thermocouples located in the fixed bed reactor. Carbon conversion was easily calculated with the information provided by the gas analyzer sampling after methanation, while the reaction temperatures were on-line registered and graphically shown by the Labview system.

The reactor was heated up to near 200 °C through electric resistances and the nitrogen flow was preheated in the ceramic furnace. Some figures of the reactor are shown elsewhere [41]. Then, the activation of the

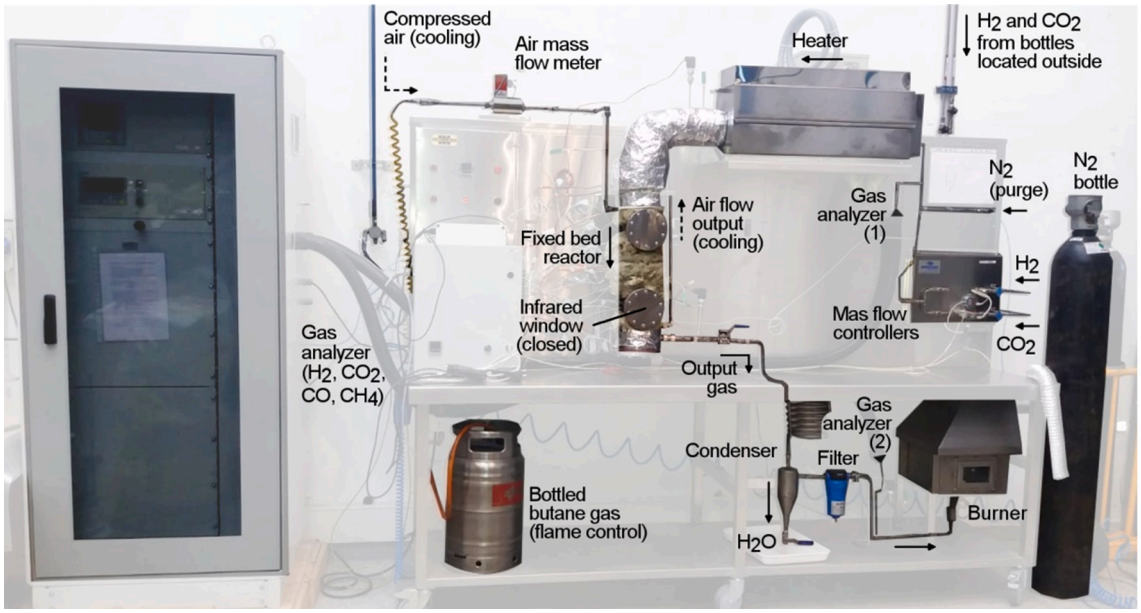

Fig. 1. Methanation test facility.

catalyst with hydrogen was carried out during 35–50 min. After that, the electric resistances were turned off and stationary states were searched under different operation conditions. The reactor was filled with 100 g of Ru-based catalyst. Ten steady operation states of methanation were established without requirements of external cooling. The main operation parameters are gathered in Table 1. In all cases the CO fraction is lower than 0.15%. In the reactor, there is temperature profile caused by the exothermic methanation reaction. The average temperature (T_a) of the methanation zone is shown in the Table 1 together with the data of these two thermocouples. No large temperature differences are observed in the reaction zone.

For stoichiometric methanation (molar H_2/CO_2 of 4.0) and ideal operation conditions, the maximum CO_2 conversion is expected to be 87.5% [41] with outlet CH_4 concentration of 58.3 %vol dry basis. The base case with stoichiometric molar ratio was established for 1 kW_{LHV}: mole flow of H_2 and CO_2 set approximately at 30.4 g/h (15.2 mol/h) and 167.2 g/h (3.8 mol/h), respectively [41]. From that case, the molar ratio is increased while keeping constant GHSV until full conversion to methane is achieved.

As it can be observed in Table 1, an experimental conversion of 81.9% was achieved in test 1, which is quite close to the equilibrium. It is necessary to emphasize that the methanation was carried out with a single reactor in a single stage and without gas recirculation. Specifically, for a ratio H/C = 4.04 the outlet flow has 50.3% by volume of methane but there is a fraction 11.1% of CO_2 in the produced synthetic gas, what makes it inappropriate to be injected into the network. As the H/C ratio increases, so does the conversion of carbon dioxide. In these experimental tests, the amount of hydrogen supplied was maintained approximately constant, increasing the H/C ratio through the proper reduction of the CO_2 injected into the mixture. In these experiments, the molar fraction of CH_4 in the produced synthetic gas decreases as expected because of the scarcity of CO_2. However, the objective of these tests is not to reach the maximum conversion rate, but to reduce the CO_2 concentration in synthetic what in fact is observed. Under all of these conditions the temperature of the reactor remained relatively constant around 350 °C.

For a ratio H/C of 5.0 the carbon conversion increases up to 95.5%. The content of CO_2 in syngas has already dropped to 2.1%, and CH_4 and H_2 volume fractions are 44.1% and 53%, respectively. Finally, for a ratio H/C of 6.4, a total conversion of carbon is achieved and any trace of CO and CO_2 in the synthetic gas produced is removed. In such case, the concentrations of CH_4 and H_2 are 30.4% and 69.5%, respectively. This operating point is the objective pursued in this work. The injection of the synthetic gas in the natural gas network will have fewer limitations than the injection of the same flow of pure H_2.

From H/C ratio of 5.0 to 6.4 there are intermediate points with impurities (mainly CO_2 concentration) in the synthesis gas between 0 and 2%. The case of H/C ratio of 5.65 is interesting as the CO is completely eliminated and the CO_2 content is less than 0.1% while there is a significant concentration of CH_4 close to 36%. The results show that with a

Table 1
Summary of experimental conditions and results.

Test			Input Mass						Output Mole Fraction (dry basis)		
	Molar H_2/CO_2	GHSV (l/h/gr)	H_2 (g/h)	CO_2 (g/h)	T_r (°C)		T_a (°C)	CO_2 Conv. (%)	CH_4 ($\%_{vol}$)	CO_2 ($\%_{vol}$)	H_2 ($\%_{vol}$)
1	**4.04**	4.21	30.1	164.1	345	370	**358**	81.89	50.9	11.3	37.9
2	**4.21**	4.33	31.1	161.1	342	360	**351**	84.45	48.9	9.0	41.4
3	**4.39**	4.36	31.7	159.0	338	360	**349**	89.14	49.8	6.1	44.1
4	**4.46**	4.26	31.1	153.3	346	356	**351**	89.98	49.2	5.5	45.3
5	**4.76**	4.23	31.2	144.3	343	366	**354**	93.05	49.3	3.7	47.0
6	**5.00**	4.47	33.3	146.4	350	369	**359**	95.45	44.5	2.1	53.4
7	**5.28**	4.48	33.6	140.0	353	365	**359**	97.52	41.9	1.1	57.0
8	**5.65**	4.35	33.0	128.6	346	351	**348**	99.92	36.1	0.0	63.9
9	**5.73**	4.51	35.6	121.3	345	370	**358**	100.00	30.3	0.0	69.7
10	**6.38**	4.47	34.5	119.0	342	360	**351**	100.00	30.4	0.0	69.5

technically simple and economically feasible methanation stage, CO_2 can be used to reduce the limitations to the injection of renewable energy via H_2 in the natural gas network.

A thermodynamic simulation of the process has been carried out to find from which H/C ratio a conversion of 100% can be obtained. Fig. 2 shows that, for the reactor and the conditions considered in the experimental tests, this relationship is about 5.5. Assuming a H_2 production from 1 kW_{LHV} (1.33 to 1.53 kW_e power depending on electrolyzer efficiency) which corresponds to about 34 g/h of H_2, the CO_2 required according the experimental tests and simulation results would be 136 g/h. The use of a 300 kW_e electrolyzer (65% LHV efficiency [49]) would result in a hydrogen production of 71 Nm^3/h which would allow a CO_2 utilization of about 21.9–24.7 kg/h (depending on the H/C ratio) to produce between 8 and 9 kg/h of CH_4 (11.7–12.5 Nm^3/h) respectively. This amount of synthetic natural gas would be injected into the network along with the excess of produced H_2. These figures were used to simulate the injection of the mixture in the gas grid.

3. Gas network model

The transient and multi-component simulation of the renewable gas injection within a gas network infrastructure has been carried out using the in-house gas network model developed by Cavana et al. and described and validated in [33]. The approach for the transient fluid-dynamic modelling of a fluid network is widely described in the literature (e.g.[50]) and may be summarized in the following general steps:

1) application of the conservation equations of mass, momentum and energy to a single pipeline or pipeline section;
2) linearization of the partial differential set of equations;
3) extension to the whole network infrastructure by means of matrix representation of network topology.

As it is commonly accepted within the gas sector, the simulation is carried out by assuming an isothermal gas flow condition [51], thus the application of the energy conservation equation can be avoided, reducing the size of the problem.

In order to be able to assess blending scenarios, the natural gas has been modeled as a mixture of 21 chemical species (including light hydrocarbons, hydrogen, carbon dioxide etc.) which can vary in space and in time. The physical properties of the mixture has been determined by using the GERG 2008 equation of state [52]. In [53], the mathematical formalization of the fluid-dynamic model is fully explained. It is also reported here in Appendix, together with the description of the quality tracking section.

The possible variations in the natural gas composition throughout the network due to distributed injection of unconventional gases may be simulated thanks to a dedicated quality tracking section of the gas network model based on the so-called “batch method” approach as described in [54]. This method have been extended to be applied on to a whole network structure in [33].

The gas network model takes as inputs the thermal request at each external node, which represents a final user or a cluster of users. The injection nodes may be regulated in pressure or in gas flow. In this case, the pressure is set at the node corresponding to the “fossil” natural gas inlet, which correspond to the city-gate pressure reduction station where the natural gas, coming from the transmission level of the network is reduced in pressure and it is delivered to the distribution infrastructure. The node in which the injection of unconventional gas will take place is instead regulated in gas flow.

Dealing with a multi-component and quality tracking simulation, the gas rate request at each consumption node is updated according to the calorific value of the gas, which depends on the gas quality. The fluid dynamic problem is then solved iteratively in order to take into account the updated gas quality composition at each node until convergence is reached.

4. Gas grid simulation

In order to assess the positive effect that methanation may play on the grid injection of renewable gases, a gas grid simulation framework has been set up. The availability of a 300 kW electrolyzer with a conversion efficiency of 65% LHV has been assumed. This electrolyzer size produces an amount of hydrogen that equals about the 4% of the energy request of the whole area for the considered day. It allows to obtain a hydrogen flow rates which, in case of direct network injection in the framework of the chosen case study, causes an already significant impact on the gas quality within the network, as it will be discussed later on in the paper.

The following injection cases have been addressed:

1. 100% H_2 injection case:
   The resulting 6.4 kg/h of hydrogen is directly injected and blended into the natural gas system.
2. 63.9/36.1 H_2/CH_4 injection case (SNG from experiment 8 - H/C ratio: 5.65):
   The resulting 6.4 kg/h is instead feed into the methanation system which is run with a H/C ratio of 5.65. The resulting SNG, whose composition is 63.9 $\%_{mol}$ H_2 and 36.1 $\%_{mol}$ CH_4, is directly injected and blended into the natural gas system.
3. 69.5/30.4 H_2/CH_4 injection case (SNG from experiment 10 - H/C ratio: 6.38):
   The resulting 6.4 kg/h is instead feed into the methanation system which is run with a H/C ratio of 6.38. The resulting SNG, whose composition is 69.5 $\%_{mol}$ H_2 and 30.4 $\%_{mol}$ CH_4, is directly injected and blended into the natural gas system.

In the following, a short description of the gas network addressed for these simulations is given.

4.1. Gas grid description

The gas network addressed in this work is based on a real network asset serving a small municipality located in Northern Italy. It covers a surface of about 29 km^2 with a population of approximately 6500 inhabitants. The total number of active gas meters in the area is equal to 3262, of which 94% are classified as residential or tertiary users’ gas meters while the remaining 6% are classified as industrial users’ ones. The annual gas consumption of the area is equal to 6.4 tons. The network is served by a single city-gate booth and the whole infrastructure works on three pressure levels. According to the information shared by the network operator, the pressure set-point is 4.98 bar_g. For the sake of this work, the simulations have been limited to the higher pressure level (medium pressure level). A schematic of the network topology is given in Fig. 3. In terms of topology, the network is weakly meshed due to the presence of two loops. This is a common design feature of medium pressure distribution gas network. This level of the gas infrastructure has a total length of about 34 km and it is made of pipelines with nominal diameter ranging from 25 mm to 280 mm.

According to [55], the Italian regulatory framework sets the upper limit for medium pressure network to 5 bar_g while for the Spanish case this value is 4 bar_g. A set-point pressure of 4 bar_g has been chosen so that it could be representative for both the countries. This set point is set at the outlet of the city-gate reduction station, corresponding to node 1 of Fig. 3.

Concerning temperature, as the problem has been developed over isothermal assumption, the gas inside the pipe has been assumed to be in thermal equilibrium with the external environment, so $T = 288.15$ K was assigned. Gas temperature variation may be registered at pressure reduction stations. However, these are usually equipped with pre-heating system to regulate the outlet temperature to the ambient one recovering the temperature decrease due to Joule-Thomson effect. In any case, the network model does not consider within the modelling

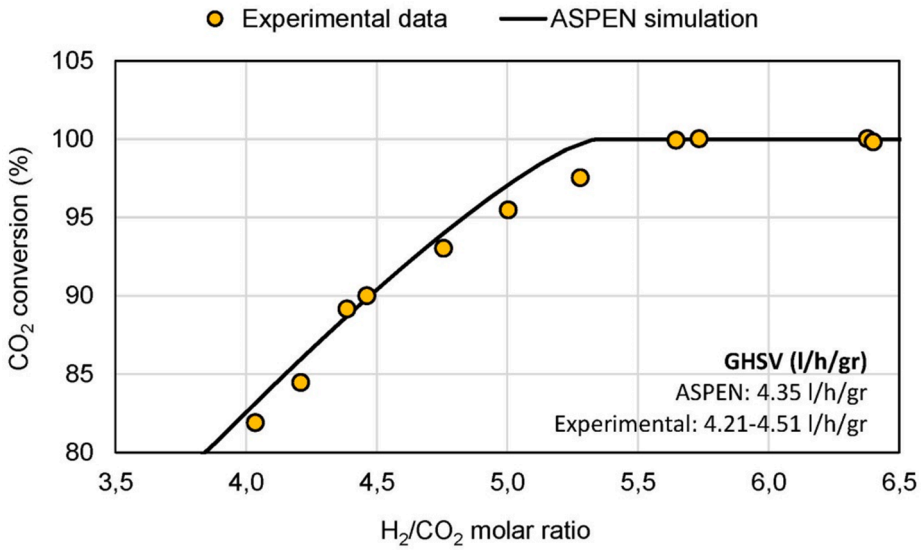

Fig. 2. Comparison between ASPEN simulation and experimental results.

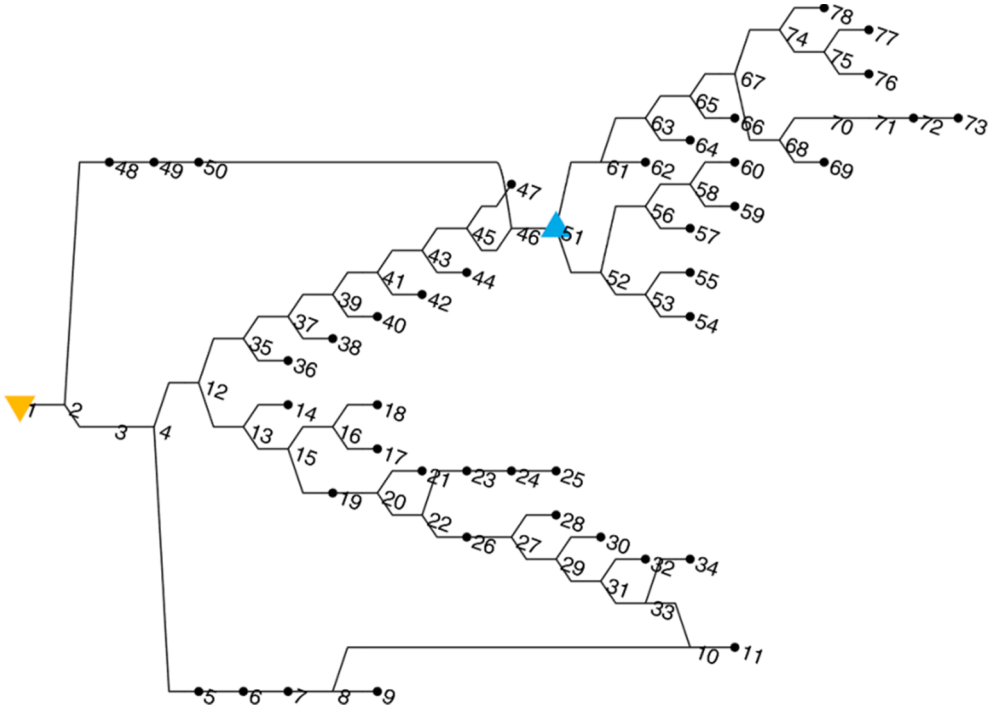

Fig. 3. Medium pressure topology of the gas distribution network.

domain the pressure regulators in this context.

Concerning the natural gas composition, it has been assumed that the fossil gas feeding the network is the Algerian one, whose main specifications are given in Table 2. The Algerian gas is the main gas serving Spain with about the 75% of share [56] and it is also present in Italy, as Algerian gas contributes to the 18.8% of the Italian gas imports [57].

In order to carry out fluid-dynamic simulations of the gas network, the gas consumption rates of all the connected users have to be known with a suitable time resolution. Due to the lack of smart and telemetered gas counters, the only available data on gas consumption is the yearly consumption of each user. Starting from the available data, the profiling procedure has been performed as detailed in [59], based on the Italian standard profiling methodology which takes into account two different type of users (residential and industrial), three types of weekly usage and accounts for the seasonality of the heating season. In this way, consumption pattern with an hourly resolution have been obtained. To furtherly refine the time resolution to 5 min time step (the resolution adopted in this work) linear interpolation has been used.

The following network simulations have been run on a one-day-long time interval, choosing a representative day of gas network usage, corresponding to an average consumption working day (mid-season gas consumption conditions). The daily gas consumption of the whole area is equal to 10,677 kg of natural gas

To assess the impact of the distributed injection of renewable gases, an injection node located in the middle of the network has been chosen, node 51, as highlighted in Fig. 3. For all the three injection cases described in the next paragraphs, the injection of the unconventional gas (hydrogen or SNG) starts at the beginning of the simulation time

Table 2
Typical natural gas composition and gas quality parameter for the Algerian gas [58].

Chemical species		Algerian Gas [% mol/mol]
Methane		86.486
Ethane		8.788
Propane		1.179
Iso Butane		0.085
Normal Butane		0.107
Iso Pentane		0.021
Normal Pentane		0.015
Hexane +		0.017
Nitrogen		1.323
Carbon Dioxide		1.894
Helium		0.085
Oxygen		–
Gas quality parameter	units	
Higher Heating Value	[MJ/Sm^3]	39.841
Wobbe Index	[MJ/Sm^3]	49.992
Relative Density	[–]	0.6351

interval, thus it is possible to track the quality perturbation as the unconventional gas substitutes the fossil one.

4.2. Base case H_2 injection into the gas grid. Limitations.

This first injection scenario aims to assess the impact of pure hydrogen injection within the natural gas infrastructure. Table 3 summarizes all the data that are relevant to this injection case.

Fig. 4 gives a network-wide overview of the impact of the distributed injection of hydrogen in a gas distribution infrastructure in a specific timestep of the simulation.

The choice of the node, as well as the topology of the network have a role in determining the area of the network that might be affected by the injection. In this specific case, all the nodes downstream the injection point will receive a certain amount of hydrogen. Fig. 5 reports the variation over time of the three gas components that are relevant to this work: methane, hydrogen and carbon dioxide.

Two sampling nodes have been chosen so to highlight the transport of the quality perturbation through the network. As it is possible to see, at the injection node (node 51) the blending of hydrogen takes place at the moment the injection starts while Node 78 receives the quality perturbation with a constant lag for the whole day. The resulting hydrogen molar fraction at the beginning of the blending is about 24%. The concentrations of methane and carbon dioxide are in turn modified, passing from 86.5% to around 65.6% and from 1.9% to around 1.4% respectively. The dashed line at 2.5% on the CO_2 concentration graph indicates the explicit limit on the carbon dioxide presence that is expressed both in the Spanish and in the Italian technical regulation on gas quality [27,28].

Even though the hydrogen injection has been assumed as constant, its share within the natural gas changes over the day. This is due to the gas consumption pattern of the gas users downstream the injection node: as the gas needs increase, the amount of fossil natural gas passing through the injection point increases thus the hydrogen fraction decreases. Under these circumstances, the hydrogen share varies between 17.5% and 26.0%. To stabilize the hydrogen fraction to a fixed amount, the injection rate should be modulated according to the downstream consumption rates.

Table 3
Relevant data for the pure hydrogen injection case.

Test	Electrolyzer			Grid Injection
	P_ren input (kW)	η_{LHV}	H_2 output (kg/h)	INPUT TO THE GRID H_2 (kg/h)
0	300	65%	6.4	6.4

Contrary to the case of CO_2, there are no specific limits to hydrogen concentration within the natural gas both in the Spanish and in the Italian technical regulation and network codes on gas quality. In the gas network codes of Spain [27] and Italy [28], the natural gas entering the gas system is required to be within specific ranges of three main quality parameters: relative density, higher heating value and Wobbe Index[1]. In Table 4 these values are given for the Spanish and the Italian case, as specified in [27,28].

Given that the hydrogen presence within the natural gas has an impact on the value of the three quality parameters, a hydrogen-blending limit may be defined as the smallest share of hydrogen that causes one of the three gas quality parameters to be out of the acceptability range. Fig. 6 displays the change of relative density, higher heating value and Wobbe index of the Algerian natural gas-hydrogen blends, as the share of hydrogen increases. The shaded areas show the acceptability range of each parameter for both the Italian and the Spanish case as detailed in Table 4.

It is possible to note that the Spanish network regulation allows much broader ranges for natural gas Wobbe index than the Italian one, thus enabling the network to host up to 33% of hydrogen (against the 21% of the Italian case). However, the relative density is the most limiting parameter, reducing the acceptable hydrogen share to 14.2% both for the Spanish and for the Italian framework.

It is worth to highlight that network regulations quality requirements usually applies to the gas that is to be injected into the network, thus just before the injection point (although some EU countries allow injection of pure hydrogen [29]). In this way, the quality compliance of the gas flowing within the infrastructure is always granted. Thus, the direct injection of pure hydrogen and/or any other unconventional gas which does not meet the gas quality requirement is forbidden, even though the blending potential of the network (i.e. the balances of gas flows) would be so to generate a mixture which is still compliant with the regulations. In this work, the gas quality requirement restrictions are moved from upstream to downstream the injection point, thus allowing unconventional gases injection as long as the gas quality is preserved on a network-wide level.

Under these premises, the hydrogen level that is reached during the case of pure hydrogen injection within a portion of gas network is well above the limit of 14.2%, thus making the direct injection strategy not acceptable.

4.3. Proposed $CH_4 + H_2$ injection into the gas grid

The methanation pathway is here tested as a method to lower the impact of pure hydrogen injection within the gas network. Starting from the same amount of green hydrogen flow rate, two cases of methanation are considered for the gas network simulation. The relevant data are summarized in Table 5.

With respect to the previous case, the methanation of a portion of hydrogen to methane leads to a lower volume of gas to be injected. The reduction is equal to 53% for test #8 (injection case A) and to 47% for test #10 (injection case B). However, the resulting syngas is made of a remarkable share of hydrogen, which exceed 60% in both cases. For what concerns CO_2, the syngas of test #8 may contain traces of CO_2 (in the order of 0.01%) given that the CO_2 conversion is not 100%.

The variation over time of the molar shares of methane, hydrogen and carbon dioxide are given in Fig. 7. The figure groups together the concentration profiles of the three relevant gas components for all the

[1] The Wobbe Index is defined as the ratio between the fuel gas heating value (higher or lower) and the square root of its relative density ($WI = HHV/\sqrt{RD}$), where the relative density of a gas is the ratio of the density of the gas to the density of the air both calculated at standard pressure and temperature conditions.In this work: normal conditions [$T_n = 273.15\ K, p_n = 101,325\ Pa$]; Standard conditions [$T_{STD} = 288.15\ K, p_{STD} = 101,325\ Pa$];

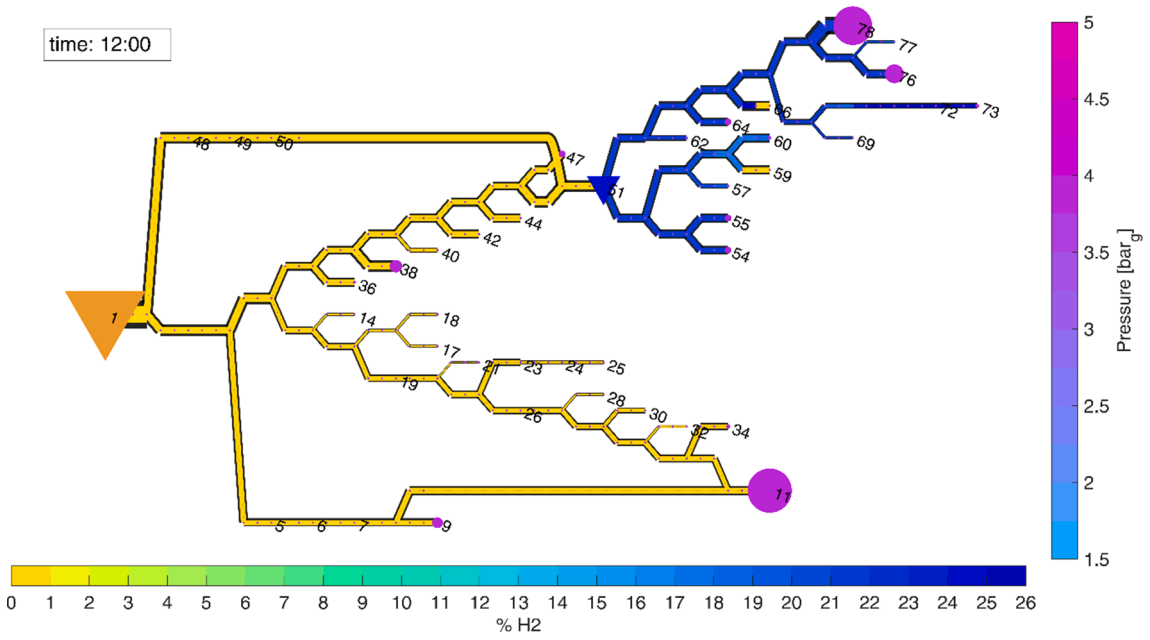

Fig. 4. Overall gas network visualization of the fluid-dynamic results of the simulation of hydrogen injection at node 51 at a specific time step (mid-day). The orange triangle (node 1) indicates the natural gas entry point; the blue triangle (node 51) indicates the hydrogen injection point. The violet "bubble" represents the gas consumption at each node (the size is proportional to the consumption flow rate). The colour indicates the level of pressure reached at each consumption node (ref: vertical indicator bar to the right). The colour of the branch indicates the share of hydrogen injected (ref: horizontal indicator bar). (For interpretation of the references to colour in this figure legend, the reader is referred to the web version of this article.)

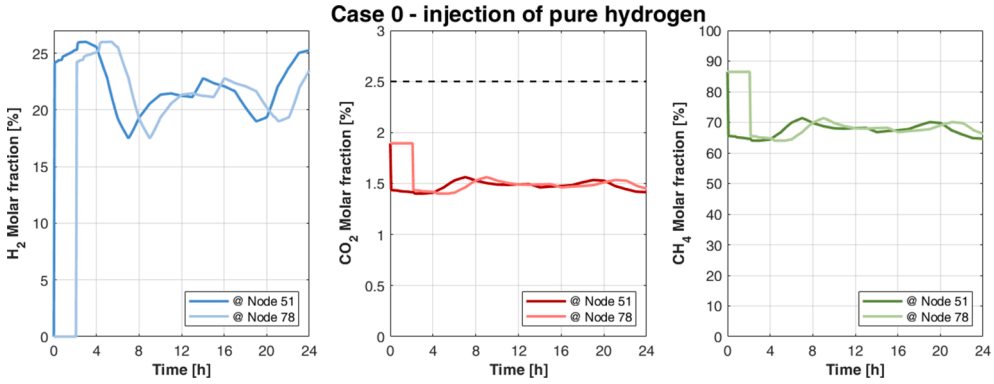

Fig. 5. Variation over the whole simulation period of the concentration of hydrogen, carbon dioxide and methane subsequent to the constant hydrogen injection. Two sampling nodes are represented: injection node (node 51) and one peripheral node (node 78 – lighter colour).

Table 4
Spanish and Italian limits on the main gas quality parameters as expressed in the network codes and regulations in [27,28] respectively. The properties are reported at the standard temperature and pressure conditions defined by ISO 13443 (i.e. $T_{STD} = 288.15\ K, p_{STD} = 101,325\ Pa$).

Property	Units	Country	Minimum	Maximum
Relative density	[–]	Spain	0.555	0.7
		Italy	0.555	0.7
Higher heating value	[MJ/Sm^3]	Spain	35.05	45.30
		Italy	34.95	45.28
Wobbe Index	[MJ/Sm^3]	Spain	45.78	56.39
		Italy	47.31	52.31

three injection scenarios tested. The graphs are arranged by column with the left one referring to the case 0–100% hydrogen injection, so to have a direct comparison of the benefits related to the methanation step. For what concerns injection scenario A (test #8), the hydrogen molar fraction ranges between 5.7% – 8.9%, always below the limit of 14.2%. Both methane and carbon dioxide shares reduce accordingly, with methane varying between 80% and 82%. In the case of test #10, the higher hydrogen content of the syngas gives a final natural gas-hydrogen admixture in the grid that displays the hydrogen share oscillating between 6.9% and 10.8%.

4.4. Comparison of results

For each of the three scenarios of distributed injection of renewable gases, a reduction of the consumption of natural gas from fossil origin is obtained. This is given in graphical form in Fig. 8, where the fossil natural gas savings are given both in mass absolute terms (left axis) and in relative terms with respect to the daily consumption in the case where no injections are performed (right axis). Referred to the simulation presented here, the daily consumption of natural gas for the case of no injection of renewable gases is 10,645 kg/day, corresponding to 151.4 MWh per day. Even though differences among renewable gases injection cases are small, the highest savings of fossil natural gas occur when pure hydrogen is injected, being equal to 3.8%. Between the two cases of

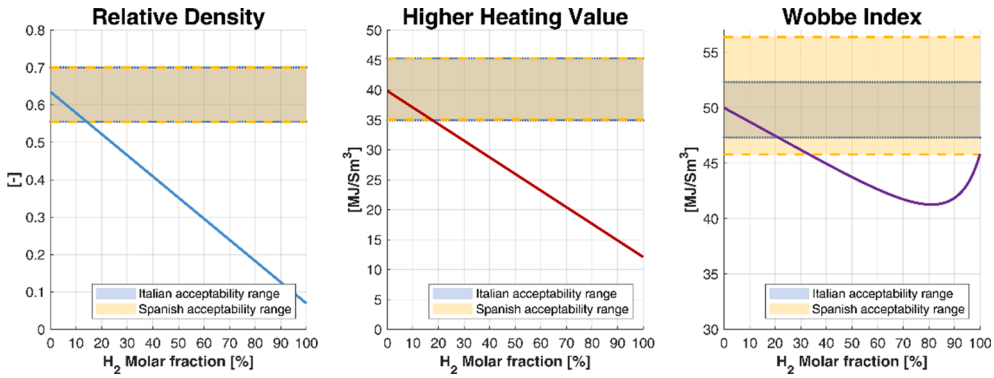

Fig. 6. Change of relative density, higher heating value and Wobbe index of the Algerian natural gas-hydrogen blends, as the share of hydrogen increases.

Table 5
Relevant data for the SNG injection cases.

Test	Electrolyzer		Methanation					Grid Injection		
				Input Mass			Output Gas/ Input to the Grid	Mole Fraction (dry basis)		
	P_Ren input (kW)	H_2 output (kg/h)	molar H_2/CO_2	H_2 (kg/h)	CO_2 (kg/h)	CO_2 Conv. (%)	$CH_4 + CO2 + H_2$ (kg/h)	CH_4 ($\%_{vol}$)	CO_2 ($\%_{vol}$)	H_2 ($\%_{vol}$)
8 / A	300	6.4	**5.65**	6.4	24.7	99.92	10.9	36.1	0.0	63.9
10 / B	300	6.4	**6.38**	6.4	21.9	100.00	10.4	30.4	0.0	69.5

injection of SNG, case B is the one which allow a higher saving (equal to 3.4%) while case A is the lowest one (3.2%). It is interesting to note that case A is also the case in which the amount of residual hydrogen in the SNG is the lowest. Thus, the injection of pure hydrogen allows a slightly higher saving in terms of fossil natural gas utilization. The reason is to be found in the higher heating value (on mass basis) of hydrogen with respect to natural gas or methane.

However, according to the results from the discussion about the gas quality parameters, a possible limit of the hydrogen share within the natural gas may be 14.2%. The results from the simulation of case 0, in which pure hydrogen is injected, shows that the molar fraction of hydrogen downstream the injection point oscillates between 17.6% and 26%, well above the threshold. Fig. 9 displays the difference between the injected hydrogen flow rate in case 0 and the maximum allowable hydrogen injection stream in order to comply with the blending limit of 14.2%. The red shaded area represents thus the curtailed hydrogen. The total amount of hydrogen curtailed within the simulation window is 60.4 kg, corresponding to 2.4 MWh (HHV based). This corresponds to a curtailment of 39.4% of the total produced hydrogen.

Fig. 10 shows, in energy terms, the contribution of each gas to the total gas consumption of the whole area (referred to the representative day used for the simulation), for the different scenarios compared: the base case without any injection, the case with pure hydrogen injection, and the two cases of SNG injection (A and B). In the presence of a limit on the hydrogen molar fraction within the gas network, the hydrogen contribution in energy terms must be shrunk from 3.8% to 2.2%.

In this context, then, the methanation pathways offer a viable solution to avoid renewable hydrogen curtailments. Starting from the same hydrogen flow rate produced by a 300 kW electrolyser, the non-stoichiometric methanation allows a complete use of the renewable hydrogen in order to form a hydrogen-rich SNG to be acceptably injected within the grid, thus recovering the 39.4% of renewable energy that would be curtailed in the form of excess of hydrogen.

Beyond the significant advantage of the proposed concept to increase the injection of green hydrogen into the gas network, an energy cost must be paid to implement it. The energy penalties related to the partial methanation strategy comes from two main sources: the heat released in the methanation reaction and the energy cost of producing the CO_2 fed to the reactor. Around a 20% of the chemical energy of the reacted hydrogen in the methanation reactor is invested and released in the exothermal reaction. Thus, the chemical energy content of the produced methane is only an 80% of the content of the reacted hydrogen. Furthermore, the carbon dioxide source must be taken into consideration since the carbon capture process always presents an energy penalty which must be allocated to the input CO_2 flow to the methanation reactor. This energy investment varies depending on the carbon dioxide source (e.g. from fossil fuels) and the capture process. Using current technologies and costs, the energy consumption to capture carbon ranges from 220 to 385 kWh/ton CO_2 [60]. Although this energy consumption is close to zero if oxyfuel combustion technology is selected and oxygen from electrolyser is used [3661].

To be observed that the practice of pure hydrogen blending introduces a fraction of gas that has no carbon content at all, reducing the carbon emission at the final users. The conversion of the same amount of hydrogen (assumed to be produced form renewable source) into SNG not only results in a slightly less fossil gas saving (if no hydrogen injection limits are set), but also it bounds back carbon atoms with hydrogen which will be released as CO_2 at the final user. Even though these molecules are meant to be recycled from a capturing source, the net emissions of the final users of the gas network has to account for these carbon emissions.

5. Conclusions

In this study, we proposed performing non-stoichiometric methanation (H_2/CO_2 ratio > 4) before injecting hydrogen to the gas grid, to prevent local hydrogen concentration from exceeding the limits of European regulations. This work included experimental characterization of non-stoichiometric methanation to select the optimal H_2/CO_2 ratio, and the simulation of the natural gas grid to compare the local blending when injecting pure H_2 or H_2/CH_4 mixtures from partial methanation.

The experimental tests were carried out in a fixed bed reactor containing 100 g catalyst (0.5 wt% Ru/Al_2O_3) at 350 °C and 4.35 l/h/gr gas hourly space velocity. The H_2/CO_2 molar ratio was varied between 4 and 6.4 (i.e., 1.00 to 1.15 kW of H_2), obtaining CO_2 conversions from 81.9% to 100%. Experimental conversion was also validated through

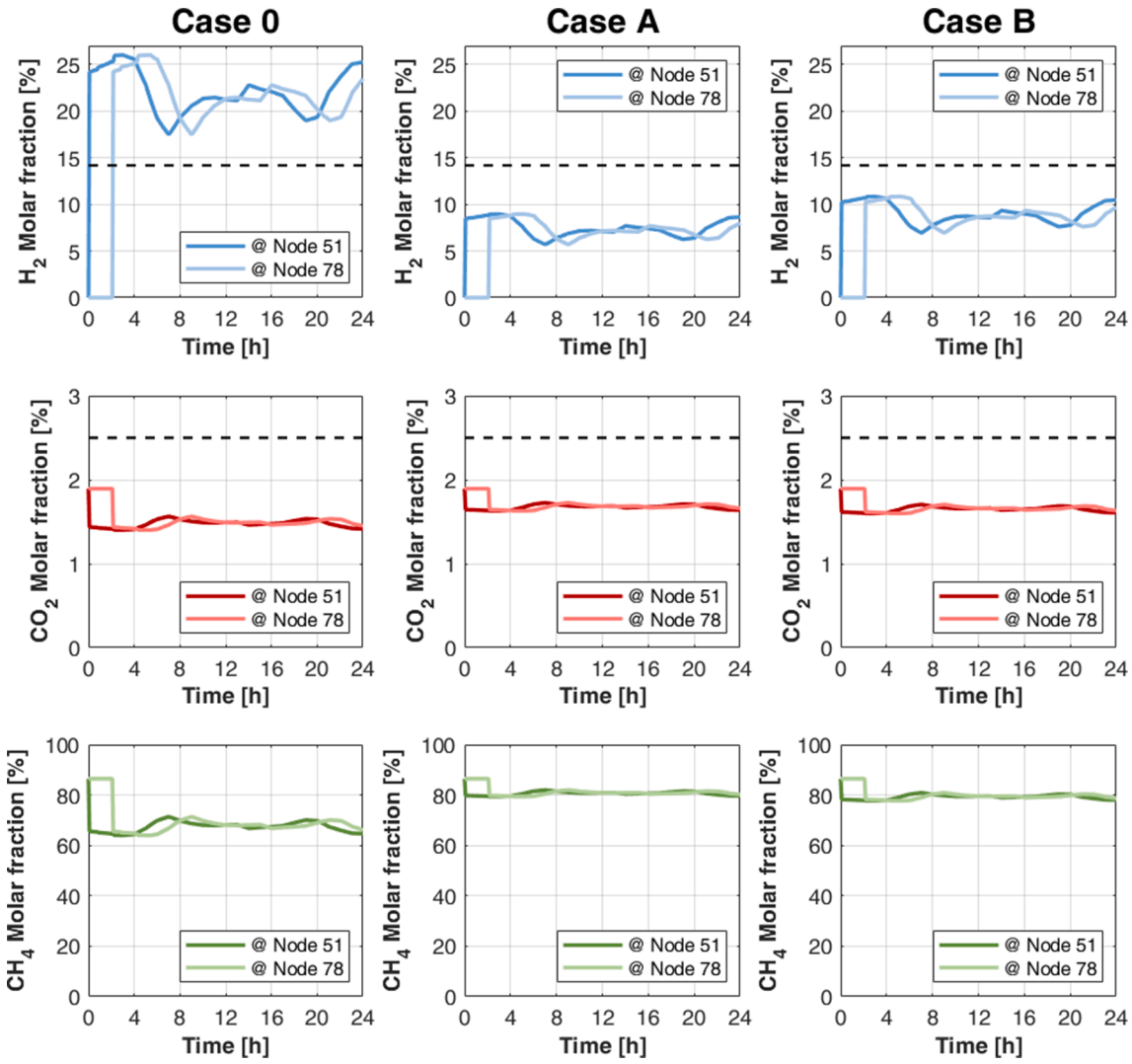

Fig. 7. Variation over the whole simulation period of the concentration of hydrogen, carbon dioxide and methane subsequent to the constant hydrogen injection (Case 0) or syngas produced from the equivalent amount of hydrogen (case A and B). The results of each simulation cases are arranged by column, to allow the comparison among the cases. Two sampling nodes are represented: injection node (node 51) and one peripheral node (node 78 – lighter colour). The dashed lines represent the acceptability limits of hydrogen and carbon dioxide concentrations.

simulation in Aspen Plus, obtaining less than 2.2% relative error. The unreacted CO_2 becomes negligible in the final mixture when the H_2/CO_2 reactants ratio is above 5.5, what is advisable due to the strict limitations on CO_2 blending (<2.5%) of European regulation. At this operating point (5.5 H_2/CO_2 ratio), 4 kg of CO_2 per kg of H_2 are required (i.e., 84 kg/h CO_2 per MW of electrolyzer, assuming 70% electrolysis efficiency). The higher the H_2/CO_2 ratio, the lower the CO_2 mass flow requirement. It should be noted that complete conversion is achieved in a single reactor, therefore the complexity of the process is reduced (design, control and operation), facilitating the economic viability of the concept.

To assess the beneficial effect of injecting H_2/CH_4 mixtures, a gas grid simulation was developed, based on a real network asset serving a population of 6500 inhabitants in Northern Italy (34 km in length). The model takes into account residential and industrial consumers, different weekly uses, and the effect of the seasons, with hourly resolution. The injection of pure H_2 was compared to the injection of synthetic gas from non-stoichiometric methanation at H_2/CO_2 ratio 5.65 and 6.38. For all the three cases, the same flow rate of hydrogen has been considered (6.4 kg/h) as produced by a 300 kW electrolyzer. The electrolyser was sized in order to provide a daily amount of hydrogen that, in energy terms, is equal to 4% of the natural gas consumption and which caused the formation of a gas blend that is non-compliant with the current gas quality requirements.

Even though most European countries (among which Spain and Italy) forbids the direct injection of pure hydrogen or any other gases which are not compliant with the gas quality requirements prior to the injection, in this work the verification of gas quality parameters has been moved downstream the injection. In this way, the direct injection of unconventional gases is allowed as long as the gas quality requirements are preserved on a network-wide level, highlighting the blending potential of the network. When it is not the case, as it is when pure hydrogen is injected, curtailment of renewable gas injection should be considered

Even though the direct injection of hydrogen would lead to the maximum fossil natural gas substitution, leading to natural gas savings of 3.8%, the resulting hydrogen blend formed in the network may be not acceptable in terms of gas quality parameters. Considering a limiting value of the acceptable hydrogen concentration of 14.2% (so that the resulting hydrogen-natural gas blend would be compliant with the actual gas quality requirements), the curtailment from the gas network injection of the 39.4% of the produced hydrogen would be required, reducing the natural gas savings to 2.2%. If instead the same hydrogen amount would be used in a non-stoichiometric methanation step, the

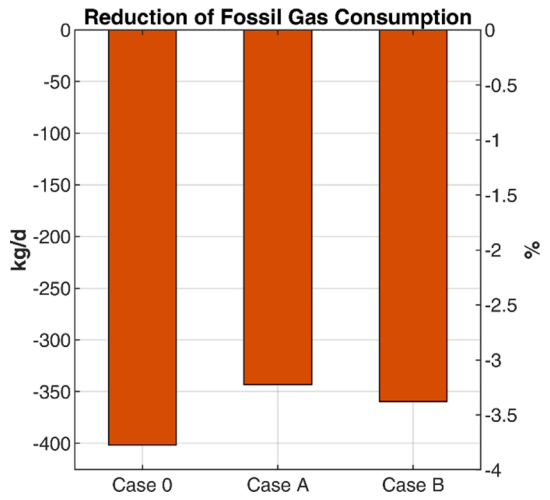

Fig. 8. Reduction of fossil natural gas consumption in the three cases of distributed injection of renewable gases. Left axis: daily mass absolute reductions; right axis: percentage of reduction with respect with the base case where no injections are performed.

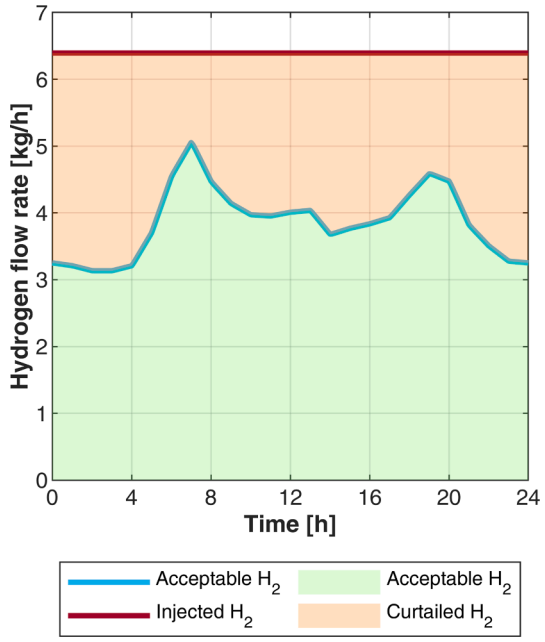

Fig. 9. Hydrogen curtailment in case of in the case of 14.2% of hydrogen limit on the natural gas composition. The red curve represents the constant hydrogen injection flow rate related to the steady production from 300 kW electrolyzer. The blue curve represents the allowable hydrogen flow rate to create a blending with a constant hydrogen fraction of 14.2%. The red area represents the curtailed hydrogen. (For interpretation of the references to colour in this figure legend, the reader is referred to the web version of this article.)

resulting SNG (which is a mixture of methane, hydrogen and carbon dioxide) can be fully accepted within the network, leading to natural gas savings of 3.2% (case A) and 3.4% (case B), without saturating the hydrogen acceptability of the gas network. However, this additional methanation step requires an extra energy cost related to the heat losses in the exothermal methanation reaction and to the energy penalty associated to the CO_2 flowrate required in the methanation step. These energy penalties in the methanation reaction itself achieve around 20% of hydrogen energy content but it can be used as thermal. With regard to the carbon dioxide consumption, the energy cost achieves could be reduced to zero using oxygen with oxyfuel combustion technology. The

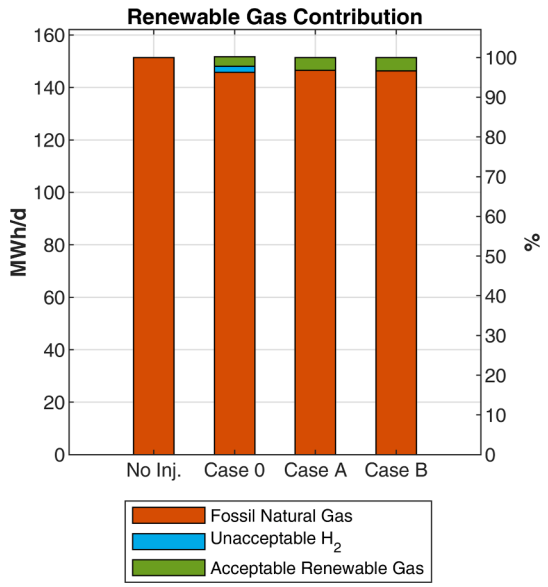

Fig. 10. Renewable gas (either green hydrogen or SNG) contribution to the total gas consumption of the network on the simulated representative day for all the scenarios addressed. The share of unacceptable hydrogen is highlighted in light blue to show the impact of possible limitation to the hydrogen molar fraction within natural gas. (For interpretation of the references to colour in this figure legend, the reader is referred to the web version of this article.)

obtained results prove the benefits of the proposed concept for injecting hydrogen into the gas grid avoiding potential curtailments by injecting renewable gas in the form of synthetic gas obtained through non-stoichiometric methanation. However, on a regulatory base, the injection of unconventional gases (containing from high fraction to 100% hydrogen) is still banned by most of national regulatory authorities [29]. A discussion on local and international gas quality requirements and on the strategies for its control and management should be carried out in light of grid accessibility and of the safe and efficient network management.

CRediT authorship contribution statement

Luis M. Romeo: Conceptualization, Formal analysis, Funding acquisition, Investigation, Methodology, Project administration, Resources, Supervision, Validation, Writing – original draft, Writing – review & editing. **Marco Cavana:** Conceptualization, Formal analysis, Investigation, Methodology, Software, Validation, Visualization, Writing – original draft, Writing – review & editing. **Manuel Bailera:** Formal analysis, Investigation, Resources, Software, Validation, Visualization, Writing – original draft. **Pierluigi Leone:** Conceptualization, Formal analysis, Investigation, Resources, Software, Supervision, Writing – original draft. **Begoña Peña:** Formal analysis, Investigation, Resources, Software, Validation, Visualization, Writing – original draft. **Pilar Lisbona:** Formal analysis, Investigation, Resources, Software, Validation, Visualization, Writing – original draft.

Declaration of Competing Interest

The authors declare that they have no known competing financial interests or personal relationships that could have appeared to influence the work reported in this paper.

Acknowledgments

The work described in this paper is supported by the R + D Spanish National Program from Ministerio de Economía y Competitividad,

MINECO (Spanish Ministry of Economy and Competitiveness) and the European Regional Development Funds (European Commission), under project ENE2016-76850-R. Authors would like to acknowledge the use of Servicio General de Apoyo a la Investigación-SAI, Universidad de Zaragoza.

Appendix. Gas network model equations assuming an isothermal gas flow it is possible to neglect the energy conservation equation so to reduce to two the equations of the set of PDEs:

Conservation of Mass

$$\frac{\partial \rho}{\partial t}+\frac{\partial(\rho v)}{\partial x}=0 \tag{1}$$

Conservation of Momentum

$$\frac{\partial(\rho v)}{\partial t}+\frac{\partial(\rho v^2)}{\partial x}+\frac{\partial p}{\partial x}+\frac{\lambda \rho v|v|}{2D}+\rho g sin\alpha=0 \tag{2}$$

Where:

- ρ: fluid density $[kg/m^3]$;
- v: fluid velocity $[m/s]$;
- p: fluid pressure $[Pa]$;
- λ: friction factor $[-]$
- D: pipeline diameter $[m]$;

The friction factor λ being calculated through an explicit approximation of Coolebrook-White equation by Cheng [58]. In order to close the mathematical formulation of the problem, the equation of state for real gas has been considered:

Real Gas Law:

$$\frac{p}{\rho}=Z\frac{R_0}{MM}T \tag{3}$$

Where:

- Z: compressibility factor $[-]$;
- R_0: Universal Gas Constant $[J/molK]$;
- MM: molar mass $[g/mol]$;
- T: temperature $[K]$;

The compressibility factor Z, a function of pressure and temperature, is determined through the GERG 2008 equation of state [48], a multiparameter equation of state explicit in the Helmholtz free energy. Under the assumption of multi-component gas stream, the compressibility factor Z and the molar mass will be function of the composition vector $[y]$.

3.1. Pipeline equation

When dealing with network simulations, it is convenient to substitute the velocity v with the mass flow rate $\dot{m}$ by means of the following relation:

$$\dot{m}=\rho v A \tag{4}$$

As additional simplifying assumptions, the kinetic and the gravitational terms (the second and the last terms in Eq. (2)) have been neglected as commonly assumed in literature [47], thus leading to a simplified version of the equation of conservation of momentum:

$$\frac{\partial p}{\partial x}=-\frac{1}{A}\frac{\partial \dot{m}}{\partial t}-\frac{\lambda c^2}{2DA^2p}\dot{m}|\dot{m}|-\frac{g sin\alpha}{c^2}p \tag{5}$$

Eq. (5) allows the calculation of the pressure drops along each pipe of the network, which in turn drives the gas flow rate. A linearization procedure is needed in order to generate and algebraic system of equations representing the whole network.

First, a substitution of variable is performed assuming $P=p^2$, thus referring to quadratic pressure, obtaining:

$$\frac{\partial P}{\partial x}+\frac{2g sin\alpha}{c^2}P=-\frac{2p}{A}\frac{\partial \dot{m}}{\partial t}-\frac{\lambda c^2}{DA^2}\dot{m}|\dot{m}| \tag{6}$$

The spatial derivative of Eq. (6) is integrated over the pipeline length, while the time derivative is treated by means of an implicit finite different scheme, the backward Euler method. It is one of the most common and basic numerical method for the solution of ordinary differential equations with first-order convergence and fully implicit feature, so to guarantee stability for large time steps, as reported in [59] and in [60].

The integrated form of the pipeline equation is given

$$\Delta P^{t+1}=R_I\hat{A}\cdot\left(\dot{m}^{t+1}-\dot{m}^{t}\right)+R_F\hat{A}\cdot\dot{m}^{t+1}\left|\dot{m}^{t+1}\right| \tag{7}$$

With apex t and $t+1$ indicating two subsequent time steps and with ΔP representing the quadratic pressure drop as defined here

$$\Delta P^{t+1}=P_{in}^{t+1}-P_{out}^{t+1};$$

and the coefficients of the right-hand side grouped in two resistance coefficients
$R_I = \frac{2\overline{p^{t+1}}l_e}{A\Delta t}; R_F = \frac{\lambda\overline{c^2}l_e}{DA^2} = \frac{16\lambda\overline{c^2}l_e}{\pi^2D^5}$;

representing the two physical phenomena contributing to the pressure variation along the pipeline: the inertia contribution (subscript I) and the fluid-dynamic friction (subscript F). Eq. (7) is a parabolic function of the mass flow which can be linearized assuming the linearization point as $\left(\Delta P_j^{t+1}, \dot{m}_j^{t+1}\right)$, where j is the generic pipe, as follows

$$\Delta P_j^{t+1(k+1)} - \Delta P_j^{t+1(k)} = \left.\frac{d\Delta P_j^{t+1(k)}}{d\dot{m}_j^{t+1(k)}}\right|^{(k)} \left(\dot{m}_j^{t+1(k+1)} - \dot{m}_j^{t+1(k)}\right)$$

from which, solving the derivative of the pressure drop Eq. (7), it is possible to obtain the final expression:

$$\Delta P_j^{t+1(k+1)} - \left(2R_F\hat{A}\cdot\left|\dot{m}_j^{t+1(k)}\right| + R_I\right)\dot{m}_j^{t+1(k+1)}$$

$$= -R_F\hat{A}\cdot\left|\dot{m}_j^{t+1(k)}\right|\dot{m}_j^{t+1(k)} - R_I\dot{m}_j^{t(k)} \tag{8}$$

This method was presented in [61] for the steady state case and generalized for the application to the transient equation in [46].

3.2. Gas network model

The complete algebraic model of the gas infrastructure is obtained by applying the mass conservation equation (Eq. (1)) to each node of the network (i.e. joints between two pipeline sections). Having defined a control volume around each node, the integral form of the continuity equation may be obtained as follows:

$$\frac{V_i}{c^2}\frac{dp_i}{dt} = -\sum_j a_{i,j}\dot{m}_j - \dot{m}_{ext_i} \tag{9}$$

with:

$$V_i = \frac{\pi}{8}\sum_j D_j^2\Delta x_j;$$

that is the geometrical volume of the i-th node.

Introducing the concept of incidence matrix defined as follows:

$$\mathbf{A} = \left[a_{i,j}\right]^{n\times b}, \quad a_{i,j} = \begin{cases} +1, & \text{node } i \text{ is the inlet of pipe } j \\ -1, & \text{node } i \text{ is the outlet of pipe } j \\ 0, & \text{node } i \text{ and pipe } j \text{ have no connections} \end{cases} \tag{10}$$

where n is the number of nodes (connection between pipes) and b is the number of pipe as a way to express any network topology in matrix form, it is possible to express Eqs. (8) and (9) in matrix form as follows:

$$\mathbf{A}^t\boldsymbol{P}^{t+1(k+1)} - \mathbf{R}\dot{\boldsymbol{m}}^{n+1(k+1)} = -\mathbf{R}_\mathbf{F}\left(\left|\dot{\boldsymbol{m}}^{n+1(k)}\right|^\circ\dot{\boldsymbol{m}}^{n+1(k)}\right) - \mathbf{R}_\mathbf{I}\dot{\boldsymbol{m}}^{n(k)} \tag{11}$$

$$\Phi\boldsymbol{p}^{n+1} + \mathbf{A}\dot{\boldsymbol{m}}^{n+1} + \mathbf{I}\dot{\boldsymbol{m}}_{ext}^{n+1} = \Phi\boldsymbol{p}^n \tag{12}$$

This set of equations are to be solved simultaneously for each time step of the simulation period, provided that suitable boundary conditions at the gas pipeline inlet and outlet are assigned. Usually, the pressure at the inlet node of the network is fixed and kept constant for the whole simulation time while the gas out-take is assigned at the outlet nodes (final users or clusters of users). Because of the linearization of the pipeline equation, for each timestep the fluid-dynamic problem will be solved iteratively until the residue of the pipeline equation will be smaller than a given tolerance (usually 10^{-4}).

3.3. Quality tracking

The tracking of the gas with different composition throughout the network requires two different methodologies: one dedicated to the motion of the gas along the pipes and the other to solve the mixing problem at network nodes.

The quality tracking along the pipes is solved using the so-called "batch method" as described in [50]: the transport equation of the composition vector [y]

$$\frac{\partial y_{(c)}}{\partial t} + v\frac{\partial y_{(c)}}{\partial x} = 0 \tag{13}$$

is treated in a Lagrangian approach in which the system of coordinates is integral with a control volume of the fluid. Each control volume should have

invariant mass and composition, while the density changes according to the expansion or the compression of the volume itself. The tracking method in the Lagrangian approach consists in the determination of the new position of each batch at every time step:

$$b_h^{t+1} = b_h^t + v_j^t \Delta t \tag{13}$$

Where b_h^{t+1} is the coordinate of the batch, v_j is the gas velocity in the j^{th} pipe element, which has been computed from the solution of the hydraulic problem.

The determination of the composition vector $[y]$ for each node of the network is given by the solution of the mixing problem at the junctions where more than two pipes connects. The continuity equation (Eq. (9)) is applied to the nodal control volume for each gas component (c) of the gas mixture, for each single chemical species. The set of resulting equation is detailed in [33].

The gas rate request at each consumption node is updated according to the calorific value of the gas, which depends on the gas quality. The fluid dynamic problem is then solved again in order to take into account the updated gas quality composition at each node.

References

[1] Nadeem F, Hussain SMS, Tiwari PK, Goswami AK, Ustun TS. Comparative review of energy storage systems, their roles, and impacts on future power systems. IEEE Access 2019;7:4555–85. https://doi.org/10.1109/ACCESS.2018.2888497.

[2] Martín M, Grossmann IE. Optimal integration of renewable based processes for fuels and power production: Spain case study. Appl Energy 2018;213:595–610. https://doi.org/10.1016/j.apenergy.2017.10.121.

[3] Bailera M, Lisbona P, Romeo LM, Espatolero S. Power to Gas projects review: Lab, pilot and demo plants for storing renewable energy and CO_2. Renew Sustain Energy Rev 2017;69. https://doi.org/10.1016/j.rser.2016.11.130.

[4] Abbess J. Renewable Gas. The Transition to Low Carbon Energy Fuels. Palgrave Macmillan UK 2015. https://doi.org/10.1057/9781137441805.

[5] Götz M, Lefebvre J, Mörs F, McDaniel Koch A, Graf F, Bajohr S, et al. Renewable Power-to-Gas: A technological and economic review. Renew Energy 2016;85:1371–90. https://doi.org/10.1016/j.renene.2015.07.066.

[6] Speirs J, Balcombe P, Johnson E, Martin J, Brandon N, Hawkes A. A greener gas grid: What are the options. Energy Policy 2018;118:291–7. https://doi.org/10.1016/j.enpol.2018.03.069.

[7] Mazza A, Bompard E, Chicco G. Applications of power to gas technologies in emerging electrical systems. Renew Sustain Energy Rev 2018;92:794–806. https://doi.org/https://doi.org/10.1016/j.rser.2018.04.072.

[8] European Commission. A hydrogen strategy for a climate-neutral Europe - COM (2020) 301. COM(2020) 301 2020.

[9] Enagás, Energinet, Fluxys Belgium, Gasunie, GRTgaz, NET4GAS, et al. European Hydrogen Backbone; 2020.

[10] Melaina MW, Antonia O, Penev M. Blending Hydrogen into Natural Gas Pipeline Networks: A Review of Key. Issues 2013.

[11] Quarton CJ, Samsatli S. Power-to-gas for injection into the gas grid: What can we learn from real-life projects, economic assessments and systems modelling? Renew Sustain Energy Rev 2018;98:302–16. https://doi.org/10.1016/j.rser.2018.09.007.

[12] Messaoudani ZL, Rigas F, Binti Hamid MD, Che Hassan CR. Hazards, safety and knowledge gaps on hydrogen transmission via natural gas grid: A critical review. Int J Hydrogen Energy 2016;41(39):17511–25.

[13] Pluvinage G. Mechanical properties of a wide range of pipe steels under influence of pure hydrogen or hydrogen blended with natural gas. Int J Press Vessel Pip 2021;190:104293. https://doi.org/10.1016/j.ijpvp.2020.104293.

[14] EIGA. Hydrogen transportation pipelines; 2004.

[15] Dodds PE, Demoullin S. Conversion of the UK gas system to transport hydrogen. Int J Hydrogen Energy 2013;38:7189–200. https://doi.org/10.1016/j.ijhydene.2013.03.070.

[16] Huszal A, Jaworski J. Studies of the impact of hydrogen on the stability of gaseous mixtures of THT. Energies 2020;13(23):6441. https://doi.org/10.3390/en13236441.

[17] Marcogaz. Odorisation of Natural Gas and Hydrogen Mixtures; 2021.

[18] Haeseldonckx D, Dhaeseleer W. The use of the natural-gas pipeline infrastructure for hydrogen transport in a changing market structure. Int J Hydrogen Energy 2007;32(10-11):1381–6.

[19] Polman E, de Laat H, Stappenbelt J, Peereboom P, Bouwman W, de Bruin B, et al. Reduction of CO2 Emissions By Adding Hydrogen To Natural Gas; 2003.

[20] Morante JR, Andreu T, García G, Guilera J, Torrell M, Tarancón A. Hidrógeno: Vector energético de una economía descarbonizada. Fundación NATURGY; 2020.

[21] Jaworski J, Kułaga P, Blacharski T. Study of the effect of addition of hydrogen to natural gas on diaphragm gas meters. Energies 2020;13(11):3006. https://doi.org/10.3390/en13113006.

[22] GRTgaz. Report on the impact of renewable gases, and mixtures with natural gas, on the accuracy, cost and lifetime of gas meters. Literature overview for renewable gases flowmetering; 2020.

[23] Zivar D, Kumar S, Foroozesh J. Underground hydrogen storage: A comprehensive review. Int J Hydrogen Energy 2021;46(45):23436–62. https://doi.org/10.1016/j.ijhydene.2020.08.138.

[24] UNI/EN. UNI 16726:2018; 2018.

[25] Italian Ministry of the Interior. D.M. 18/05/2018 - Regola tecnica sulle caratteristiche chimico fisiche e sulla presenza di altri componenti nel gas combustibile; 2018.

[26] IEA. Current limits on hydrogen blending in natural gas networks and gas demand per capita in selected locations; 2020.

[27] Goverment S. Protocolo de detalle PD-01 «medición, calidad y odorización de gas». Bol Del Estado 2011:39355–7.

[28] Snam Rete Gas. Codice di Rete - Specifica Tecnica sulle Caratteristiche Chimico-fisiche e sulla Presenza di Altri Componenti nel Gas Naturale e nel Biometano; 2020.

[29] Agency for the Cooperation of Energy Regulators. ACER Report on NRAs Survey - Hydrogen, Biomethane, and Related Network Adaptations. Ljubljana; 2020.

[30] Abeysekera M, Wu J, Jenkins N, Rees M. Steady state analysis of gas networks with distributed injection of alternative gas. Appl Energy 2016;164:991–1002. https://doi.org/10.1016/j.apenergy.2015.05.099.

[31] Pellegrino S, Lanzini A, Leone P. Greening the gas network – The need for modelling the distributed injection of alternative fuels. Renew Sustain Energy Rev 2017;70:266–86. https://doi.org/10.1016/j.rser.2016.11.243.

[32] Cavana M, Mazza A, Chicco G, Leone P. Electrical and gas networks coupling through hydrogen blending under increasing distributed photovoltaic generation. Appl Energy 2021;290:116764. https://doi.org/10.1016/j.apenergy.2021.116764.

[33] Cavana M. Gas network modelling for a multi-gas system. Politecnico di Torino 2020.

[34] Cavana M, Leone P. Assessment of the hydrogen receiving potential of a distribution gas network using a multi component and transient gas network model. Porc 8th Eur Fuel Cell Piero Lunghi Conf, Naples 2019:311–2.

[35] Abanades JC, Rubin ES, Mazzotti M, Herzog HJ. On the climate change mitigation potential of CO $_2$ conversion to fuels. Energy Environ Sci 2017;10(12):2491–9. https://doi.org/10.1039/C7EE02819A.

[36] Romeo LM, Bailera M. Design configurations to achieve an effective CO2 use and mitigation through power to gas. J CO_2 Util 2020;39:101174. https://doi.org/10.1016/j.jcou.2020.101174.

[37] Antenucci A, Sansavini G. Extensive CO_2 recycling in power systems via Power-to-Gas and network storage. Renew Sustain Energy Rev 2019;100:33–43. https://doi.org/10.1016/J.RSER.2018.10.020.

[38] Clegg S, Mancarella P. Storing renewables in the gas network: Modelling of power-to-gas seasonal storage flexibility in low-carbon power systems. IET Gener Transm Distrib 2016;10(3):566–75.

[39] Deymi-Dashtebayaz M, Ebrahimi-Moghadam A, Pishbin SI, Pourramezan M. Investigating the effect of hydrogen injection on natural gas thermo-physical properties with various compositions. Energy 2019;167:235–45. https://doi.org/10.1016/J.ENERGY.2018.10.186.

[40] Schiebahn S, Grube T, Robinius M, Tietze V, Kumar B, Stolten D. Power to gas: Technological overview, systems analysis and economic assessment for a case study in Germany. Int J Hydrogen Energy 2015;40(12):4285–94. https://doi.org/10.1016/j.ijhydene.2015.01.123.

[41] Bailera M, Peña B, Lisbona P, Marín J, Romeo LM. Lab-scale experimental tests of power to gas-oxycombustion hybridization: System design and preliminary results. Energy 2021;226:120375. https://doi.org/10.1016/j.energy.2021.120375.

[42] Moioli E, Gallandat N, Züttel A. Model based determination of the optimal reactor concept for Sabatier reaction in small-scale applications over Ru/Al2O3. Chem Eng J 2019;375:121954. https://doi.org/10.1016/j.cej.2019.121954.

[43] Moioli E, Mutschler R, Züttel A. Renewable energy storage via CO2 and H2 conversion to methane and methanol: Assessment for small scale applications. Renew Sustain Energy Rev 2019;107:497–506. https://doi.org/10.1016/J.RSER.2019.03.022.

[44] Perna A, Moretti L, Ficco G, Spazzafumo G, Canale L, Isola MD. SNG Generation via Power to Gas Technology: Plant Design and Annual Performance Assessment. Appl Sci 2020;10:8443.

[45] Schaaf T, Grünig J, Schuster MR, Rothenfluh T, Orth A. Methanation of CO2 - storage of renewable energy in a gas distribution system. Energy Sustain Soc 2014;4:29.

[46] Gruber M, Weinbrecht P, Biffar L, Harth S, Trimis D, Brabandt J, et al. Power-to-Gas through thermal integration of high-temperature steam electrolysis and carbon dioxide methanation - Experimental results. Fuel Process Technol 2018;181:61–74. https://doi.org/10.1016/j.fuproc.2018.09.003.

[47] Lefebvre J, Bajohr S, Kolb T. A comparison of two-phase and three-phase CO2 methanation reaction kinetics. Fuel 2019;239:896–904. https://doi.org/10.1016/j.fuel.2018.11.051.

[48] Bailera, M, Peña, B, Lisbona, P, Marín, J, Romeo LM. Lab-scale experimental tests of Power to Gas- Oxycombustion hybridization: System design and preliminary results. In: 33rd International Conference on Efficiency, Cost, Optimization, Simulation and Environmental Impact of Energy Systems E 2020, editor. ECOS 2020 - Proc. 33rd Int. Conf. Effic. Cost, Optim. Simul. Environ. Impact Energy Syst.; 2020. p. 1376–87.
[49] IEA. The Future of Hydrogen. Seizing today's opportunities; 2019.
[50] Pambour KA, Bolado-Lavin R, Dijkema GPJ. An integrated transient model for simulating the operation of natural gas transport systems. J Nat Gas Sci Eng 2016; 28:672–90. https://doi.org/10.1016/j.jngse.2015.11.036.
[51] Osiadacz AJ, Chaczykowski M. Comparison of isothermal and non-isothermal pipeline gas flow models. Chem Eng J 2001;81(1-3):41–51. https://doi.org/10.1016/S1385-8947(00)00194-7.
[52] Kunz O, Klimeck R, Wagner W, Jaeschke M. The GERG-2004 Wide-Range Equation of State for Natural Gases and other mixtures. VDI-Verlag; 2007.
[53] Cavana M, Leone P. Solar hydrogen from North Africa to Europe through greenstream: A simulation-based analysis of blending scenarios and production plant sizing. Int J Hydrogen Energy 2021;46(43):22618–37. https://doi.org/10.1016/j.ijhydene.2021.04.065.
[54] Chaczykowski M, Sund F, Zarodkiewicz P, Hope SM. Gas composition tracking in transient pipeline flow. J Nat Gas Sci Eng 2018;55:321–30. https://doi.org/10.1016/j.jngse.2018.03.014.
[55] CEER. Benchmarking Report on the Quality of Electricity and Gas Supply - 05. Gas - Technical Operational Quality; 2016.
[56] Statista.com. Volume of natural gas imported by Spain in 2020, by country of origin; 2020.
[57] Italian Ministry of Economic Development. La Situazione Energetica Nazionale nel 2019; 2020.
[58] Snam. Snam - Portale Misura. MisuraSnamIt n.d.
[59] Cavana M, Leone P. Towards renewable gases distribution networks: The importance of a transient and multi-component fluid-dynamic gas model. Eur Biomass Conf Exhib Proceedings 2019:1754–61.
[60] Vasudevan S, Farooq S, Karimi IA, Saeys M, Quah MCG, Agrawal R. Energy penalty estimates for CO2 capture: Comparison between fuel types and capture-combustion modes. Energy 2016;103:709–14. https://doi.org/10.1016/j.energy.2016.02.154.
[61] Bailera M, Lisbona P, Romeo LM. Power to gas-oxyfuel boiler hybrid systems. Int J Hydrogen Energy 2015;40(32):10168–75. https://doi.org/10.1016/j.ijhydene.2015.06.074.